LASER INTERFEROMETER GRAVITATIONAL WAVE OBSERVATORY

LIGO Laboratory / LIGO Scientific Collaboration

Version 0.9	ADVANCED LIGO	T050035-02-D	2/28/05

Advanced LIGO Pre-stabilized Laser Conceptual Design Document

M. Frede, P. King (Ed.), R. Savage, R. Wilhelm, B. Willke

Distribution of this document:
LIGO Science Collaboration

This is an internal working note
of the LIGO Project.

California Institute of Technology
LIGO Project – MS 18-34
1200 E. California Blvd.
Pasadena, CA 91125
Phone (626) 395-2129
Fax (626) 304-9834
E-mail: info@ligo.caltech.edu

Massachusetts Institute of Technology
LIGO Project – NW17-161
175 Albany St
Cambridge, MA 02139
Phone (617) 253-4824
Fax (617) 253-7014
E-mail: info@ligo.mit.edu

LIGO Hanford Observatory
P.O. Box 1970
Mail Stop S9-02
Richland WA 99352
Phone 509-372-8106
Fax 509-372-8137

LIGO Livingston Observatory
P.O. Box 940
Livingston, LA 70754
Phone 225-686-3100
Fax 225-686-7189

http://www.ligo.caltech.edu

1 Introduction

Early in the formulating stages of the planning of Advanced LIGO, it was envisaged that the laser power would be increased from its initial level of 10 W as it is in Initial LIGO to 200 W. At that time a single-frequency, single-mode 200-W Nd:YAG laser had not yet been developed. In 2001 the LIGO Scientific Collaboration (LSC) proposed a development plan for the Advanced LIGO Laser in which the laser groups within the LSC would strive to develop a 100-W laser that would meet a list of criteria. The decision criterion is outlined in *Memo On How to Make the AdvLIGO High Power Laser Decision* (LIGO-T020122-00-Z).

Three competing laser technologies were under active consideration:

- master-oscillator-power-amplifier with either end or edge-pumped slab amplifiers;
- injection-locked stable-unstable oscillator design based on a side-pumped slab laser head;
- injection-locked end-pumped rod oscillator.

A standard suite of tests was performed on the competing platforms and based on the results of these tests, a platform was selected to form the basis for the design of the Advanced LIGO Pre-stabilized Laser (PSL). The selection choice is detailed in *Memo on the Selection of a Laser System For the Conceptual Design Phase of the AdvLIGO PSL* (LIGO-T030065-00-R).

As a result of progress since the initial development plan was put forth and experience gained with the Initial LIGO PSL, this document supersedes the document *LIGO II Pre-stabilized Laser Conceptual Design* (LIGO-T000036-07-W).

1.1 Purpose

The purpose of this document is to present a conceptual design that shows that the requirements presented in *Pre-stabilized Laser Design Requirements* (LIGO-T050036-00-D) are reasonable and realizable.

The principal intended audience is the Advanced LIGO Detector team.

1.2 Scope

This document details the expected challenges and a conceptual design solution generated to meet the requirements presented in *Pre-stabilized Laser Design Requirements* (LIGO-T050036-00-D). It gives an overview of the PSL subsystem – what is and what is not included in the PSL subsystem, its location in the LVEA, the relationship between the PSL and other Advanced LIGO subsystems, and its features and capabilities. Schemes to implement the frequency and intensity stabilization loops are presented, along with their estimated performance levels.

1.3 Document Organization

1.3.1 Acronyms

AM	amplitude modulation
AOM	acousto-optic modulator
ASD	amplitude spectral density

CCD	charge-coupled device
CDS	Control and Data System (detector subsystem)
CIT	California Institute of Technology
COC	Core Optics Components (detector subsystem)
DC	direct current (steady state – low frequency)
EMI	electro-magnetic interference
EOM	electro-optic modulator
EPICS	Experimental Physics and Industrial Control System
GW	gravitational wave
HAM	horizontal access module
HEPA	high efficiency particulate air
HR	high reflectance
HWP	half-wave plate
IO	Input Optics (detector subsystem)
LAE	laser area enclosure
LIGO	Laser Interferometer Gravitational-wave Observatory
LSC	Length Sensing and Control (detector subsystem)
LVEA	laser and vacuum equipment area
LZH	Laser Zentrum Hannover
MIT	Massachusetts Institute of Technology
MO	master oscillator
MOPA	master-oscillator-power-amplifier
Nd:YAG	neodymium yttrium garnet
NIST	National Institute of Standards and Technology
NPRO	non-planar ring oscillator
PID	proportional-integral-derivative
PM	phase modulation
PSD	power spectral density
PSL	pre-stabilized laser (detector subsystem)
PZT	piezo-electric transducer
RF	radio frequency
RFAM	radio frequency amplitude modulation
RIN	relative intensity noise
RMS	root-mean-square
SEI	Seismic Isolation (detector subsystem)
TBD	to be determined
ULE	Ultra Low Expansion titanium silicate glass
VCO	voltage controlled oscillator

1.3.2 Applicable Documents

1.3.2.1LIGO Documents

180 W Nd:YAG Laser Specifications, LIGO-C000060-00-D

Pre-stabilized Laser Design Requirements, LIGO-T050036-00-D

Advanced LIGO Pre-stabilized Laser (PSL) Design Requirements, LIGO-T000035-W

Memo On How to Make the AdvLIGO High Power Laser Decision, LIGO-T020122-00-Z

Memo on the Selection of a Laser System For the Conceptual Design Phase of the AdvLIGO PSL, LIGO-T030065-00-R

The following LIGO documents may be of historical interest:

(Infrared) Pre-stabilized Laser (PSL) Design Requirements, LIGO-T970080-09-D

(Infrared) Pre-stabilized Laser (PSL) Conceptual Design, LIGO-T970087-04-D

(Infrared) Pre-stabilized Laser (PSL) Electronics Design Requirements, LIGO-T970115-00-C

1.3.2.2 Non-LIGO Documents

Monolithic, unidirectional single-mode Nd:YAG ring laser, Opt. Lett. 10 pp 65-67 (1985).

Spatial and temporal filtering of a 10-W Nd:YAG laser with a Fabry-Perot ring-cavity premode cleaner, Opt. Lett. 23 pp 1704-1706 (1998)

Diode-pumped Nd:YAG laser intensity noise suppression using a current shunt, Rev. Sci. Instrum. 72, pp 1346-1349 (2001).

Frequency stabilization of a monolithic Nd:YAG laser by controlling the power of the laser-diode pump source, Opt. Lett. 25, 14 (2000).

Injektionsgekoppelte diodengepumpte Nd:YAG- und Nd:YV04-Laser fuer terrestische interferometrische Gravitationswellendetektoren, Ph.D. Thesis, Ivo Zawischa

The GEO 600 laser system, Class. Quantum Grav 19, pp 1775-1781 (2002)

High power fundamental mode Nd:YAG laser with efficient birefringence compensation, Optics Express 12 pp 3581-3589 (2004)

213 W linearly polarized fundamental mode Nd:YAG ring laser, OSA Trends in Optics and Photonics (TOPS) vol. 96 and also CLEO Technical Digest 2004 paper CPDA2

1.3.3 Definition of Terms

Gaussian beam A beam of electromagnetic radiation as such as that often produced by lasers, in which the transverse electric field varies as $E = E_0 e^{-r^2/w^2}$, where w is the beam spot size.

M^2 or M value The parameter M or M^2 is a measure of the departure of a Gaussian beam from a pure TEM_{00} mode. If the mode were a pure TEM_{00} mode, then $M^2 = 1$. The beam waist divergence product for a non-TEM_{00} mode is M^2 that of a TEM_{00} mode.

Modulation index If the phase φ of the of the laser beam is represented by $\varphi = \omega_0 t + \Gamma \sin(\omega_m t)$, then the amplitude of the phase modulation, Γ, is referred to as the modulation index.

Spot size The characteristic size for a Gaussian beam, defined as the distance (radius) at which the electric field drops to $1/e$ times the value on axis.

2 System overview

2.1 Introduction

The PSL subsystem consists of the following elements:

- The *Advanced LIGO* Laser including power supplies, the cooling system and the injection locking control systems.
- A triangular pre-modecleaner (PMC) to spatially filter the laser beam, housed in a sealed vessel to reduce atmospheric pressure-induced optical path length changes and contaminations.
- The frequency stabilization control loop utilizing a rigid reference cavity suspended in vacuum on a vibration isolation stack, an electro-optic modulator for fast frequency correction, and the control of the master oscillator frequency fluctuations via feedback to the master oscillator piezo-electric actuator (PZT). Slow large range control signals will be fed back to the master temperature control actuator.
- Overall power control of the light exiting the suspended modecleaner and entering the main interferometer. This will include a high power photodetector mounted downstream of the modecleaner which needs to be mounted inside the vacuum envelope on the seismic isolation table.
- A diagnostic breadboard to analyze the spatial beam profile, free-running frequency noise and power noise of the intermediate and high power stage.
- All computers, interface cards and software needed to control the PSL and to provide data interfaces to other subsystems and the data acquisition system.

It does ***not*** include:

- Mode matching lenses or steering mirrors that are part of the Input Optics Detector Subsystem.
- Electro-optic modulators for sideband frequencies utilized outside of the PSL subsystem.

2.2 Features / Capabilities

The *Advanced LIGO* PSL conceptual design is partly based on the *Initial LIGO* PSL. It incorporates the following features.

- Wideband input for the IO frequency control actuator
- Tidal actuator for very low frequency control of laser frequency

It incorporates the following changes and improvements based on experience gained from the commissioning of the *Initial LIGO* PSL:

- The sample of the laser output beam that is directed to the frequency reference cavity is picked off ***after*** the PMC in order to improve beam quality incident on the reference cavity and suppress frequency noise induced by the PMC due to length fluctuations.

- The PMC is mounted inside a sealed container in order to eliminate atmospheric pressure- induced optical path length changes and to avoid contamination of the optics exposed to high laser power.
- The number of optical mounts is kept to a minimum and all mounts are extremely rigid in order to reduce frequency fluctuations induced by optical mount vibrations.
- Beam pipes enclosing the majority of the propagation path of both the main laser beam and the sample beam directed toward the reference cavity for frequency stabilization.
- Environmental control including an optical table enclosure with acoustic shielding and a laser area enclosure that provides a working environment with low particle counts and which enhances laser safety.
- A minimum of acoustic noises source will be allowed in the laser area enclosure. All electronic racks with cooling fans will be situated outside that room.
- The laser diodes boxes, their power supplies and cooling units will be housed in an enclosure with HEPA filters and provisions to meet laser safety requirements in the mechanical equipment room. Optical fibers will bring the pump light to the 200 W laser system. This scheme reduces the required cooling water and electrical power in the laser area enclosure and reduces the heat load of that room.

2.3 PSL Location

The PSL will be located in the vicinity of the HAM chamber that contains the suspended input optic for the modecleaner. The performance of the *Initial LIGO* PSL has been found to be adversely affected by local acoustic noise. For this reason the *Advanced LIGO* PSL will be enclosed in a sound proof enclosure. Furthermore the PSL requires a very clean and dust free environment. To ensure clean conditions especially during parallel installation of the PSL and other *Advanced LIGO* subsystems, a laser area enclosure (LAE) will be needed. To achieve a small enough particle count to install, commission and operate the high power laser the air in the laser area enclosure has to be exchanged on a regular basis by HEPA filtered air and the pressure in that room needs to be higher than in the LVEA. During science mode the fans can probably be turned off. The size of the LAE will be defined based on the available space in the LVEA and the required area for the PSL installation and maintenance.

As with the *Initial LIGO* PSL, the *Advanced LIGO* PSL shares an optical table with the IO subsystem. The optical layout on this table and the arrangement of components will be specified once the dimensions of the laser system are known.

The distribution of the PSL electronics will be guided by the EMI concept of *Advanced LIGO* and the noise and bandwidth requirements of the PSL. For installation and maintenance purposes an EPICS workstation will be placed in the LAE which is to be turned off during science runs.

The noisy chillers for the laser system will be placed in the mechanical equipment room. To reduce the heat dissipation in the LAE the power supplies of the laser diodes will be installed in the same room. This arrangement will avoid electrical disturbances of the switching power supplies in the LVEA. If consistent with laser safety requirements the laser diodes will be put close their power supplies in the mechanical equipment room as well. With “spiral metal cladding” protected optical fibers will deliver the pump light to the laser table where the light is used to pump the Nd:YAG crystals. This reduces the length of wires carrying large currents, reduces the amount of cooling water needed in the LAE and will allow to exchange laser diodes during a science run without entering the LVEA.

A laser diode enclosure is needed for laser safety and cleanliness reasons. A sketch of the distribution of the PSL components in the building can be found in Figure 1. The balloons indicate the internal and external interfaces of the PSL which will be described later.

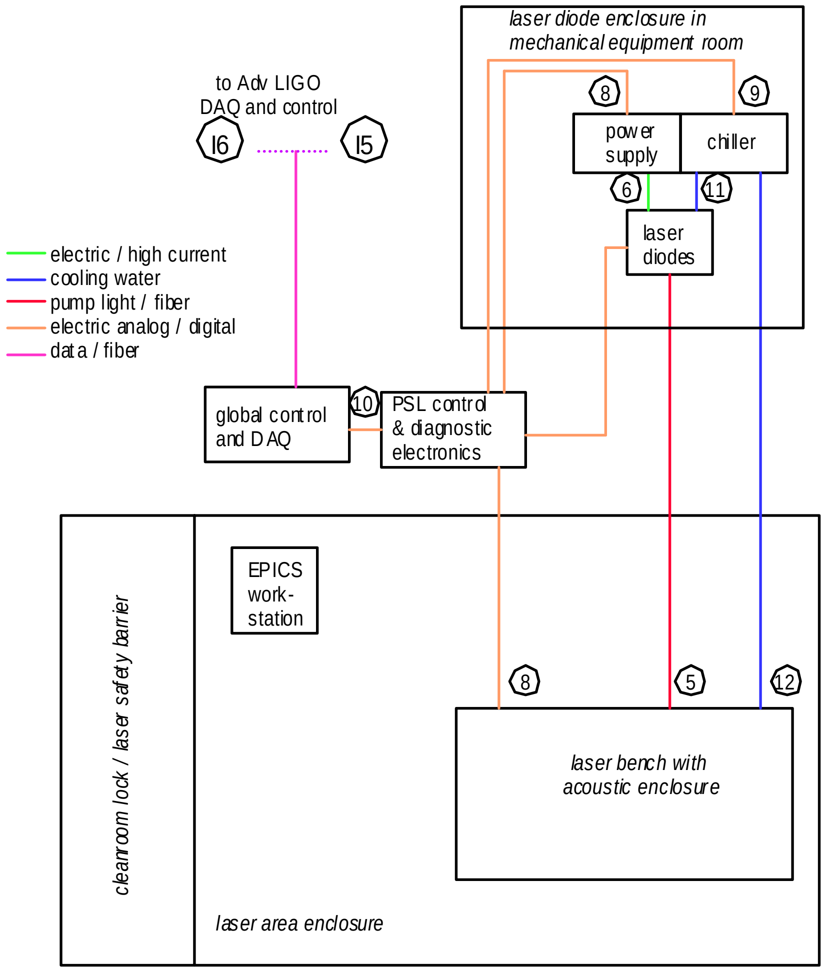

Figure 1. Arrangement of the different PSL components in the different locations: The laser bench is located in the lasers area enclosure, the control and DAQ racks are located in the LEVA outside of the laser area enclosure and the laser diodes and noisy chillers will be placed into the mechanical equipment room. (The drawing is not to scale.)

2.4 The IO / PSL Optical Table

The IO/PSL optical table is the same one that was used for the *Initial LIGO* interferometers, a 16 ft. × 5 ft. × 24 in. thick Newport Research Series table. The PSL PMC defines the beam parameter at the optical interface between the PSL and IO subsystems, which is located 30cm downstream of the PMC beam waist. The properties of the beam (waist size and position) exiting the PMC are very well defined, which makes mode matching into the modecleaner far simpler and serves to isolate beam parameter changes in the PSL from the IO. The mechanical stability of the

PMC and its support structure defines the beam pointing at the PSL – IO interface. The definition of the interface 30 cm downstream of the PMC allows us to put the pick-off point for the beam sample used for the frequency stabilization upstream of that interface. The pick-off point might be the transmission through the first turning mirror of the IO subsystem (TBD).

2.5 Laser Room

In order to enhance laser safety and to get clean room conditions, a laser room is constructed around each PSL. The dimensions of the room are similar to the size installed at LLO (24 ft. wide by 32 ft. long). The electronics racks located adjacent to the *Initial LIGO* IO/PSL optical tables are moved back to exclude them from the Laser Room. The exact position of the racks needs to be defined later according to the *Advanced LIGO* EMI standards.

2.6 Optical Layout and Control Strategy

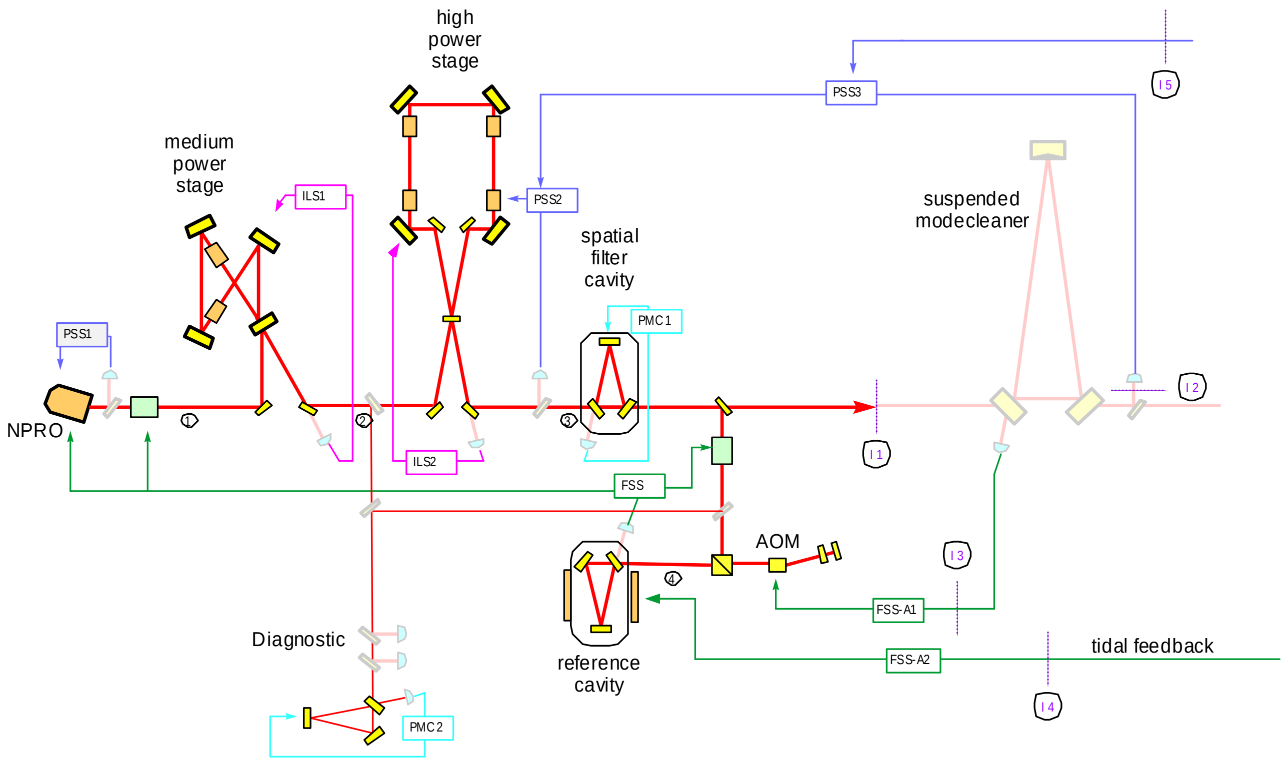

Figure 2: A schematic of the optical layout and control strategy of the PSL.

The optical layout of the PSL has four major components: the 200 W laser, a frequency stabilization path including a rigid reference cavity and an acoustic optic modulator as an actuator for the second frequency stabilization loop, a pre-modecleaner as a spatial filter and a diagnostic path that allows investigate of the laser behavior without interference with the PSL output beam. The 200 W laser consists of a master laser and two injection-locked oscillator stages. An electro-optical modulator is placed downstream of the master laser to provide a set of phase modulation sidebands that are required to produce error signals for control loops within the PSL (two injection locking loops and the PMC length stabilization). This scheme will be carefully explored during the preliminary design phase. The relation between modulation frequency and injection locking range, PM-AM conversion in the injection locking stages due to offsets and rms deviations and their propagations through the PSL etc. will be analyzed. An additional electro-optical modulator is needed in the frequency stabilization path to add the sidebands needed for the Pound-Drever-Hall sensing at the reference cavity.

The frequency stabilization scheme is similar to the *Initial LIGO* scheme. Note that the beam directed toward the reference cavity for frequency stabilization is split off from the main output beam ***after*** the PMC. This scheme has two advantages:

- The light incident on the reference cavity is closer to pure TEM_{00} mode and hence the spurious noise effects of the higher order modes on the photodetector are reduced.
- The reference cavity control loop measures and suppresses any additional frequency noise added to the beam by the PMC and all optical components, such as mirror mounts, upstream of the pick off point.

A diagnostic path will be part of the PSL that will allow for an online measurement of the beam parameters and the noise of either the 12 W intermediate power stage or the 200 W stage.

The optical train of the PSL is kept as short as practicable with the minimum number of adjustable and fixed mirror mounts. Two fixed or adjustable mounts are provided to bring the PSL output beam down to the 4” optical height utilized on the IO/PSL optical table, two adjustable mirror mounts are provided for alignment into the PMC, one adjustable mount is provided for alignment of the sample of the main beam utilized for frequency stabilization into the frequency shifter AOM and one is utilized for retro-reflection of the shifted beam back through the AOM, two adjustable mounts utilized to align the beam into the reference cavity with two fixed mirrors in a periscope raising the beam to the level required for the reference cavity. All mirrors that are simply required in order to fold the optical path for space considerations are fixed mounts. All EOMs are mounted on goniometer-type mounts that enable alignment by moving the EOM rather than steering the beam into the EOM. Lens mounts can be adjusted then locked in their final position.

2.7 Laser Safety

Laser safety is a very important consideration in the design of the *Advanced LIGO* PSL. The highest risk exists during installation, commissioning and maintenance of the high power laser system. During this phase all stray optical beams of more than 1 mW power need to be dumped. Careful planning of each work stage is required to avoid stray high power beams. Note that very high quality coatings will be required on all optical surfaces. The power transmitted when a 200 W beam is incident on an high reflectance (HR) coating with a transmittance of around 10^{-3} will be in the order of several hundred milliwatts.

Even though only trained and authorized personnel is allowed to work on the laser, stray beams are unavoidable during installation, commissioning and maintenance especially when work is performed on the high power laser and the lid of its housing is open. Hence an enclosure around the PSL table is required. This enclosure should be large enough to allow people to stand in the enclosure and work on the laser table. After the installation phase all 200 W beams will be mostly covered by metal tubes wherever this is reasonable to enhance the laser safety and to avoid falling dust particles disturbing the beam parameters. At the end of the PSL commissioning phase and after each maintenance phase all identifiable stray beams need to be blocked.

A detailed laser safety procedure document needs to be produced for the work on the PSL in the LAE.

2.8 Facilities Interfaces

The PSL will rely on the LIGO observatory facility for the supply of the mains electrical power, temperature and humidity control, and space and utilities for the laser power supplies and chillers.

2.9 Remote Control

All PSL controls will be actuated via the CDS detector subsystem. The controls inside the 200 W laser (laser diode temperature control, laser diode current control, safety and internal diagnostic) will be a stand-alone system with an interface to the CDS system. The performance of the PSL will be monitored continuously and logged to allow comparison with previous performance levels. The CDS computer will also guide the various steps in the lock acquisition sequence and will generate alarms in case of a malfunction in the PSL.

3 The Advanced LIGO Laser

3.1 Overview

The conceptual design for the *Advanced LIGO* Laser is based on an injection-locked high power ring resonator (see Figure 3). This resonator contains four end pumped laser heads, whereas each two of these heads are combined with a birefringence compensation scheme. In comparison to a MOPA scheme a stabilization of the optical resonator length is necessary. Therefore the Pound-Drever-Hall injection locking scheme will be applied. The expected advantages of an injection-locked high power oscillator are an improved beam quality, a higher overall efficiency and better noise suppression at RF frequencies. The stability requirements for the optical resonator length are given by the locking range of the oscillator which is a function of the ratio of resonator internal laser power and the power injected into the laser oscillator. Therefore, a double stage concept will be realized in order to increase the overall locking range of the system, see Section 3.3.1.

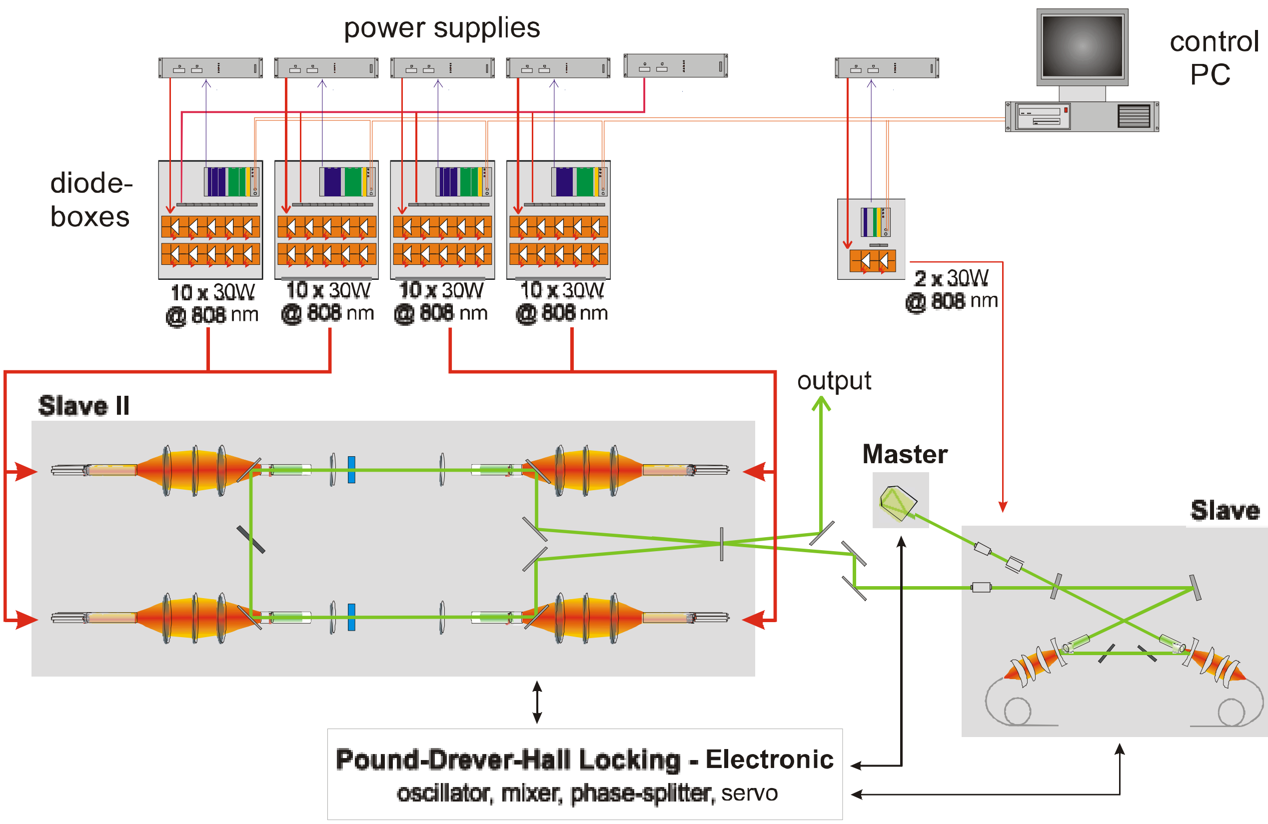

Figure 3. Schematic of *Advanced LIGO* laser showing a single-frequency master laser, an injection-locked medium power stage (Slave I) followed by the high-power stage (Slave II).

A 12 W ring oscillator (named hereafter Slave I) is frequency stabilized onto a monolithic master laser by employing the Pound-Drever-Hall stabilization scheme. In a second step, the high power oscillator (Slave II) is frequency stabilized onto the radiation field of Slave I. This concept increases the locking range of the high power laser by a factor of 4, which reduces the resonator length stability requirements for the high power laser.

3.2 Target Specifications

The *Advanced LIGO* PSL consists of a high power laser and the components used to pre-stabilize its free-running frequency and intensity. Based on the experience with a 200W testbed operated at LZH and based on the experiences in the achievable loop gain for the stabilization schemes the target requirements for the free-running laser are:

Parameter	Specification
1. type of laser	Nd:YAG
2. wavelength	1064 nm
3. power in a circular TEM_{00} mode	>200 W
4. power in all other modes	< 20 W
5. polarization extinction ratio	100:1 in the vertical plane
6. relative power fluctuations	$<10^{-3}/\sqrt{\mathrm{Hz}}$ between 0.1 Hz and 10 Hz $<10^{-5}/\sqrt{\mathrm{Hz}}$ between 10 Hz and 10 kHz $<2\times10^{-9}/\sqrt{\mathrm{Hz}}$ for $f>9$ MHz (3dB above shot noise of 50mA photocurrent)
7. frequency fluctuations	$<1\times10^{4}\ \mathrm{Hz}/\sqrt{\mathrm{Hz}}\times[1\ \mathrm{Hz}/f]$ between 1 Hz and 10 kHz (same as NPRO free running)

3.3 Laser Design

The different components of the *Advanced LIGO* Laser are described in the subsequent sections below. After introducing the injection locking technique, the front end and the high power stage are described before the laser head is introduced in detail.

3.3.1 Injection locking

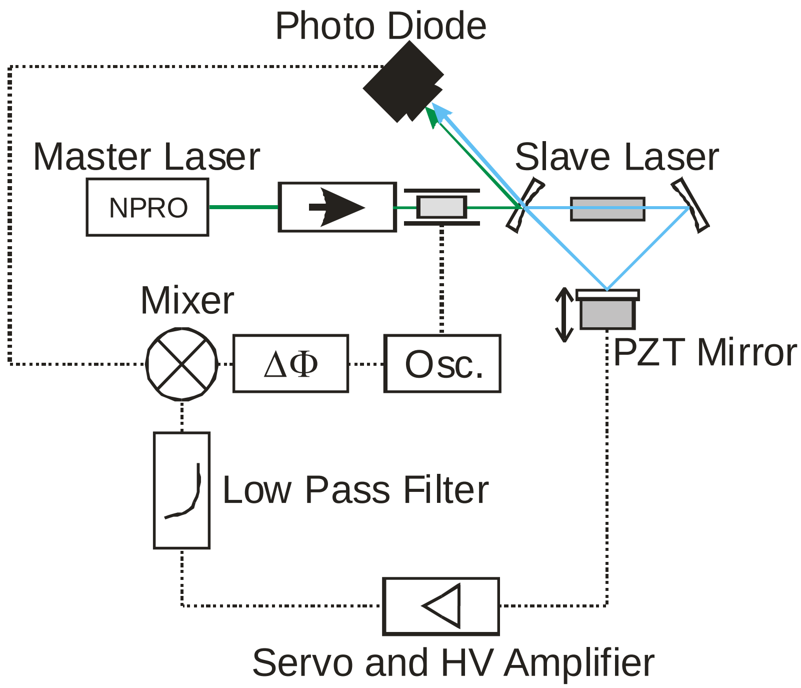

Figure 4. Schematic layout of an injection locked slave laser locked on a master laser by the Pound-Drever-Hall technique

While an injection-locked high power oscillator requires additional feedback loops for cavity length stabilization when compared to a multi-stage master oscillator/power amplifier configuration, it offers several advantages, such as

- higher overall efficiency
- better output beam quality due to intrinsic filtering by the laser's resonator
- reduced relative intensity noise at RF frequencies.

These advantages have already been demonstrated at power levels up to 25 W and are currently investigated at higher power levels up to 200 W.

The locking-range of the system is proportional to the injected master to the slave-laser power and is given by,

$$\Delta\omega = 2\gamma_e\sqrt{\frac{P_m}{P_s}},$$

where γ_e is the cavity decay rate, P_m is the injected (master laser) power and P_s is the power of the free running high power oscillator. In order to increase the locking range and reduce the requirements for the cavity length control, the ratio of the two powers should be kept low, thus requiring a double-stage scheme, while the master laser power is limited to the 1 W level.

If the frequency difference of the high power slave oscillator and the low power master laser is within the locking range, the radiation field of the master laser is being amplified by the saturable regenerative amplifier formed by the slave laser. Due to the saturation of the gain medium, unwanted laser modes do not experience sufficient gain to overcome the resonator's loss and will extinguish.

At Fourier frequencies lower than the slave laser's locking range, the phase noise characteristics are dominated by the phase fluctuations of the master laser. Resonator length fluctuations of the slave laser are more accurately described by a frequency fluctuation than a phase fluctuation. The transfer function connecting slave laser frequency noise and the phase fluctuation of the coupled system is nearly constant for Fourier frequencies below the locking range, thus meaning that resonator length changes can have an influence of the system's overall phase noise. Due to destructive interference of the beam transmitted by the cavity and the beam directly reflected at the output coupler, the amplitude transfer function takes small values at low frequencies below the locking range, so that the power noise of the system is determined by pump power fluctuations. At high frequencies larger than the inverse cavity lifetime, power noise is determined by the master laser light being reflected directly at the cavities output coupler [ref.1].

Fast and stable locking electronics enable a stable single-frequency operation. For some accidental interruption of injection locking operation *e.g.* by a strong mechanical shock to the optical table an auto-lock feature was implemented. The auto-lock applied a saw tooth voltage to the piezos which change the cavity length. If the frequency of the master and the first slave (Slave I) laser coincide, the slave laser operates in an unidirectional instead of a bidirectional mode, so that a photodiode detects a two-times higher laser output. The resultant increase of the photodiode output current triggers the servo for the Pound-Drever-Hall stabilization which locks the cavity length of Slave I to the master. If the first two systems (Master and Slave I) are locked, the second locking to the high power laser (Slave II) was started with the same procedure between Slave I and Slave II using a second photodiode and additional locking electronics. Typically the "re-lock" time of the complete system took less than 400 ms.

3.3.2 Front End

The front end for the *Advanced LIGO* Laser is based on the proven GEO600 Laser design [ref.1]. A medium power ring oscillator is injection-locked by the output radiation of a monolithic non-planar ring laser.

The medium power stage consists of a ring resonator in bow-tie configuration and involves two conductively cooled Nd:YAG crystals, each being longitudinally pumped by a fiber coupled laser diode at a derated (< 60%) output power of about 17 W. Temperature stabilization of the laser crystals and the pump diodes is performed by computer-based PID controllers.

The employment of a low thermal expansion steel for the resonator block in combination with the negation of adjustable resonator components results in a high intrinsic stability and a reduced acoustic sensitivity of the slave oscillator.

The resonator length is controlled by a piezo-electric transducer in combination with a Pound-Drever-Hall stabilization scheme.

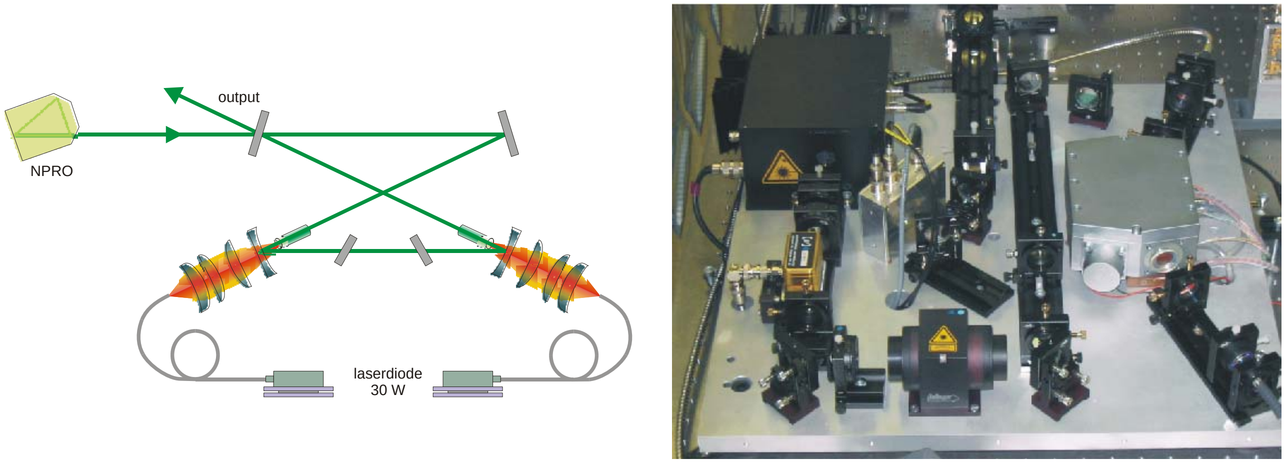

Figure 5. 12 W Front End injection-locked onto a monolithic ring laser.

3.3.3 High Power Stage

The high-power laser is based on a ring resonator design with four end-pumped laser heads, see Section 3.3.3.1. Thermally induced mechanical stress in the Nd:YAG crystals results in stress induced birefringence and causes depolarization and bifocusing. The stress induced birefringence can be compensated by involving two identically pumped rod's and a 90° quartz rotator. A relay optic consisting of two identical lenses images the principal planes of the rods onto each other while keeping the laser field unmodified. Therefore a nearly perfect birefringence compensation can be achieved [ref.2]. In the proposed *Advanced LIGO* laser, two birefringence compensated pairs are formed to a ring resonator design, see Figure 6.

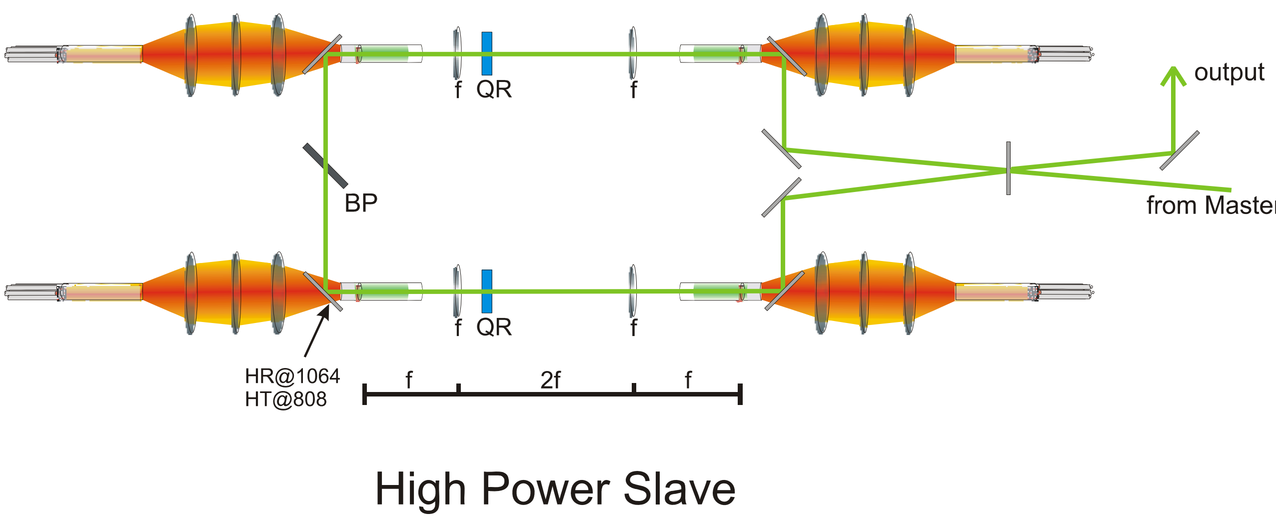

Figure 6. Schematic layout of the high power ring laser oscillator.

With this setup a laser output power of 213 W in a linear polarized fundamental mode operation was demonstrated, see [ref.3].

3.3.3.1 End pumped laser head

Each of the 4 laser crystals are pumped by 10 fiber-coupled laser diodes with a nominal power of 30 watts each and a wavelength around 807 nm. The laser diodes are individually temperature stabilized which ensures a narrow emission spectrum of the fiber bundle. Operating the laser diodes at a derated output power of about two thirds of their nominal power improves diode lifetime and reliability. The specified lifetime at full power is about 20,000 hours (27 months) during which less than a 20% increase in driving current is needed to keep the output power constant. A fused silica rod homogenizes the transverse pump light distribution due to the spatial mixing of the light rays emerging from different fibers. This ensures a nearly unchanged pump light profile in case a pump diode failure or degradation. Therefore, the failure of a single laser diode can be compensated by increasing the operating current of the remaining pump sources, while the failed diode can be replaced while operating the laser at nominal output power and beam quality. This setup reduces the risk of laser downtimes.

A three lens optic images the end surface of the homogenizer into the laser crystal (see Figure 7).

The laser crystal consists of a 3 mm diameter multi-segmented Nd:YAG rod with two 7 mm long undoped segments at both ends and a 40 mm long low-doped center segment. The undoped end caps reduce the thermally induced mechanical stress on the end surfaces of the rod and eliminate any mechanical deformation of the ends. Further on, the complete doped region of the rod can be effectively cooled, which is essential for the end-pumped geometry in connection with direct water cooling.

During propagation, the pump light is mixed and guided by total internal reflection at the rod surface. The crystal involves a double pass for the pump light in order to reduce the longitudinal thermal gradient and reduce the overall mechanical length.

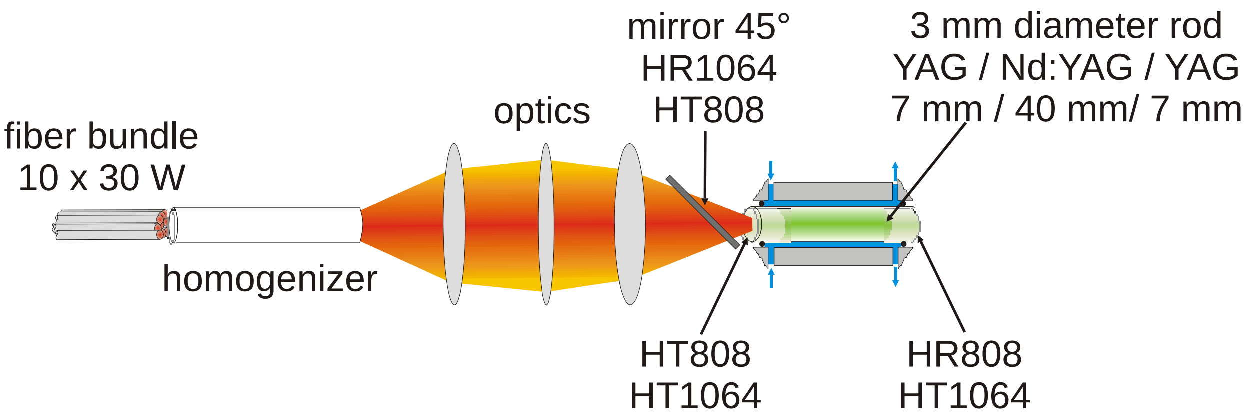

Figure 7. Schematic layout of an end-pumped laser head

The fracture stress limit of YAG ranges from 130 to 260 MPa, depending on the surface treatment of the crystal. According to a detailed theoretical thermal analysis involving a ray tracing calculation of the pump light distribution and large scale finite element modeling of the temperature distribution and resulting mechanical stresses, thermally induced von-Mises equivalent stress is below 60 MPa for the chosen crystal design (see Figure 8). Therefore, a large safety margin is being left, allowing for final optimization of the pump light distribution and its overlap with the laser-mode.

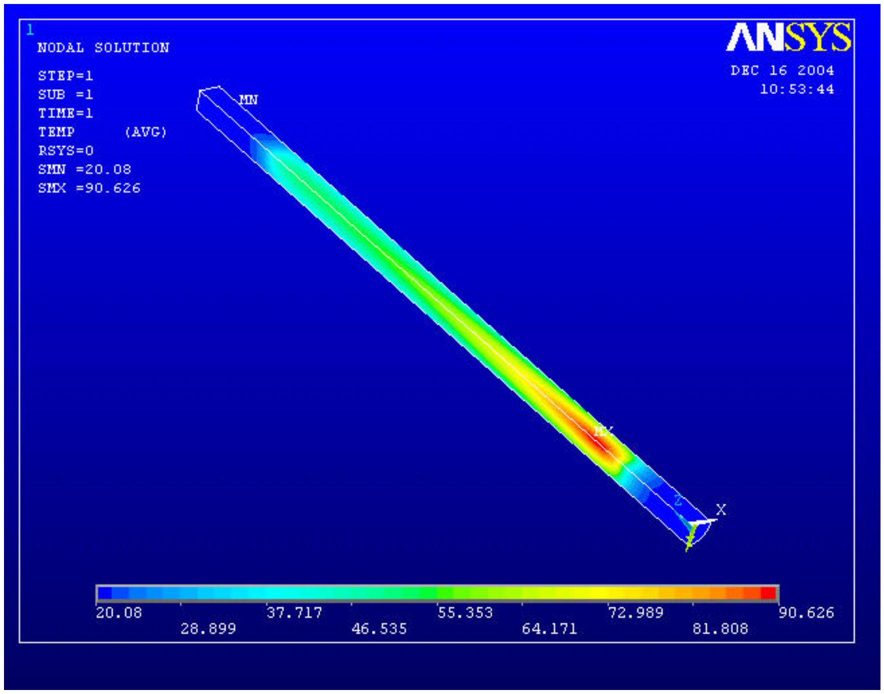

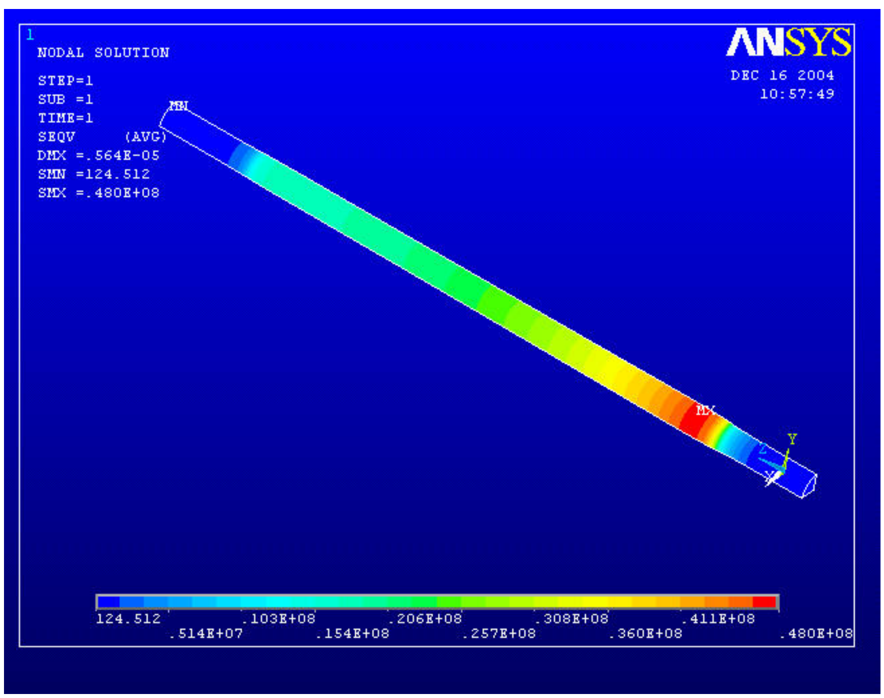

Figure 8. top: Temperature and bottom: von-Mises equivalent stress distribution in the end-pumped laser crystal at 250 W of pump power. Units are °C respectively MPa and a coolant temperature of 20 °C is assumed.

3.3.3.2 Beam quality

Scaling the laser power by increasing the pump power introduces thermally induced aberrations in the crystals due to the temperature dependence of the relevant material properties such as thermal conductivity and thermally induced refractive index changes. By keeping the average temperature in the rod below 60°C, thermally induced aberrations are drastically reduced. The second source of aberrations is the pump light distribution which concentrates near the rod-axis. By carefully optimizing the spatial overlap of pump light distribution and laser mode, the properties of the fundamental mode can be aligned to be nearly Gaussian while higher modes are suppressed by the soft aperture formed by the pump light profile.

3.3.3.3 Parasitic Oscillations

Since the power scaling is performed by increasing the number of laser rods without increasing the small signal gain per laser crystal, an onset of parasitic oscillations and the whispering gallery mode is not likely to be expected. The fact that only a medium grade surface polishing of the rod’s barrel surface is required further increases the threshold for parasitic oscillations.

3.3.3.4 Depolarization

In the current design the depolarization loss caused by thermally induced mechanical stress in the laser crystals will be greatly reduced by a birefringence compensation involving a 90° quartz rotator and a relay optic for imaging one rod’s principal plane onto the other. A reduction of total depolarization loss to less than 2% of the resonator internal power was achieved with this scheme.

3.3.4 Estimates of output properties

3.3.4.1 Output Power

An overall output power of the injection locked laser of 195 W has been demonstrated (see Figure 9).

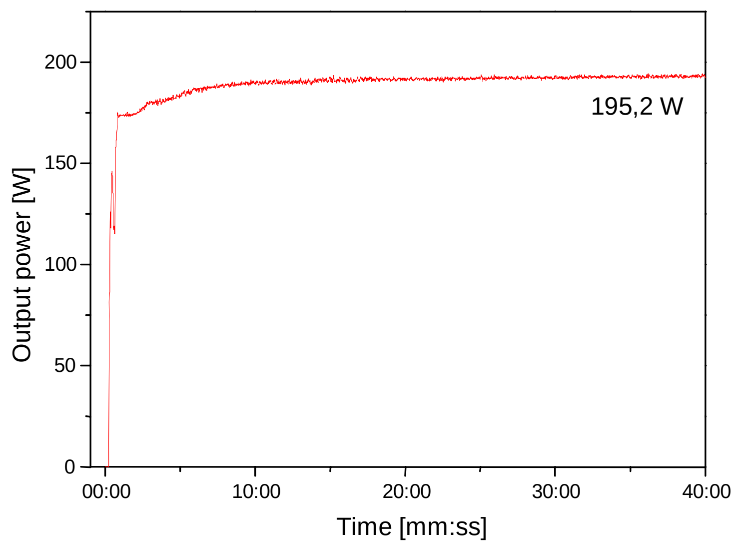

Figure 9: Output power of the injection-locked high power laser after a cold start.

3.3.4.2 RMS power noise

In measurements performed on a 100 W system the power fluctuations over 10 s where measured to be approximately 15%. If the value for the 200 W system has a similar high value the source needs to be determined and either the source or the coupling needs to be reduced to the $10^{-3}/\sqrt{\text{Hz}}$ level. Candidates for the high fluctuations are noise on the pump current for the high power stage, alignment fluctuations in the high-power oscillator cavity or fluctuations introduced by the water cooling. In case the free-running RIN below 10 Hz can not be reduced by design optimization of easy changes a trade-off between more sophisticated design changes and loop-gain in the PSL power stabilization (see Section 6) need to be made.

3.3.4.3 Power noise in the stabilization band

Figure 10 shows the relative intensity noise of Slave II. The main source for power noise at low frequencies are the pump power fluctuations. While the target specifications are not fulfilled yet, a stabilization of the pump diode current in connection with mechanical improvement of Slave II will reduce the RIN in this frequency band.

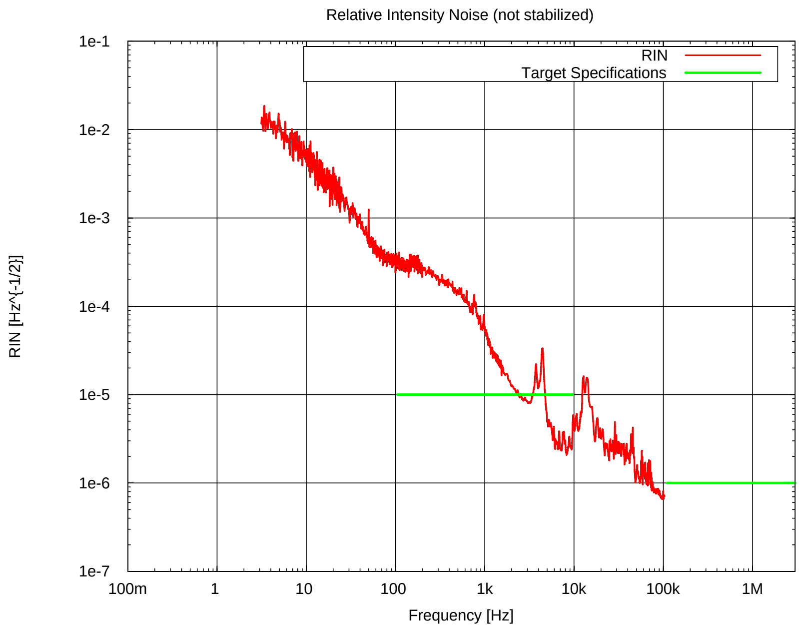

Figure 10: Relative intensity noise and target specifications in the stabilization band (Measurement on first 200W test system)

3.3.4.4 RF power noise

For frequencies above a corner frequency ω_c given by

$$\omega_c = \frac{{\omega_{rel}}^2}{\gamma_L + \Delta\omega},$$

where γ_L is the damping rate of the oscillation and depends on the stimulated emission cross section, the photon flux, the inverse lifetime of the upper laser level and the pumping rate, $\Delta\omega$ is the locking range bandwidth and ω_{rel} is the relaxation frequency, the coupling between the pump power fluctuations and the slave laser output power noise declines with a second order characteristic with increasing frequency and the power noise is dominated by the master oscillator, due to the portion of its field reflected directly at the input coupler. For parameters of the 200 W prototype laser this frequency is $\omega_c = 10\text{ kHz}$. Figure 11 shows the RIN of a GEO600 type 12 W laser which is expected to be close to the power noise of the first slave (Sascha Brozek, Diss., Hannover (1999)). Above 1 MHz the 12 W RIN is expected to dominate the 200W laser noise. A projection of the red curve indicates that the 200 W should meet the $2\times10^{-9}/\sqrt{\text{Hz}}$ requirement above 9MHz.

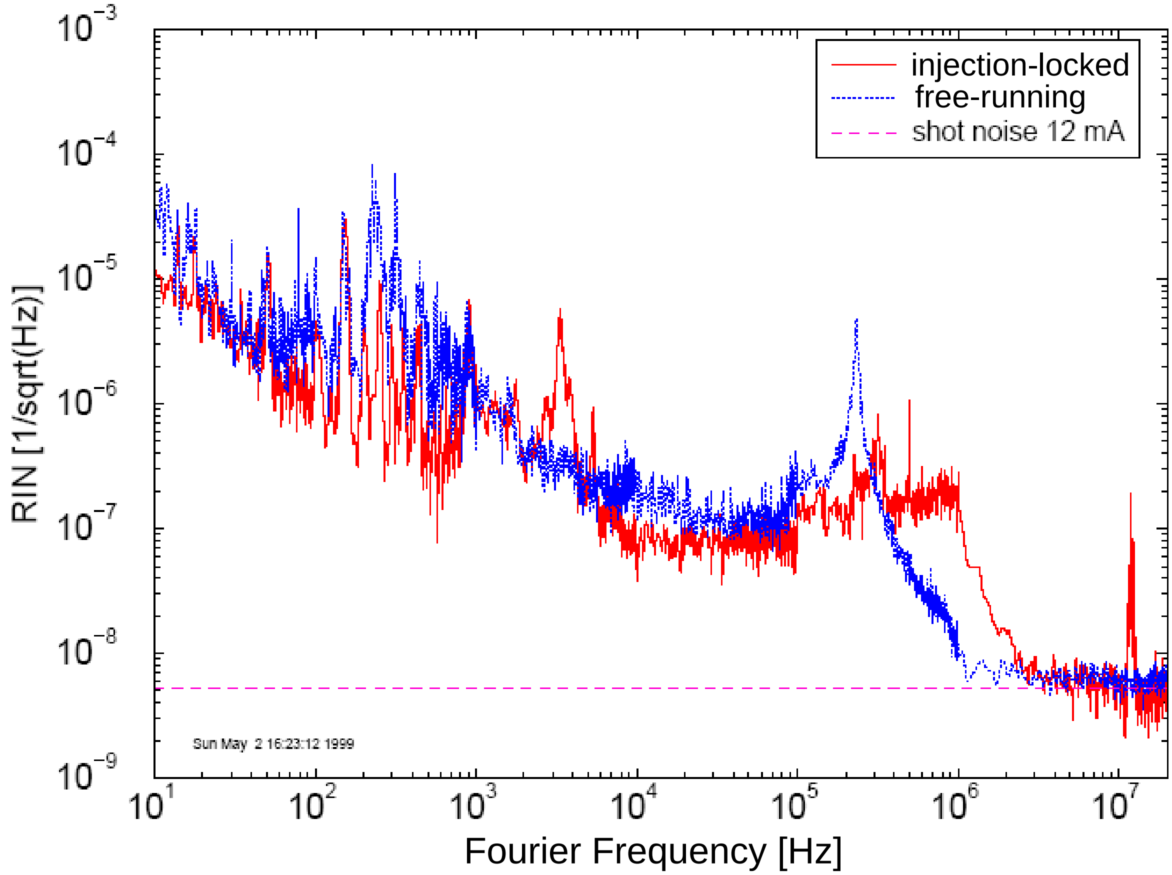

Figure 11:The relative intensity noise of a free-running and injection locked GEO600 type laser.

3.3.4.5 Frequency Noise

The frequency noise has not yet been characterized. For frequencies well below the locking range, the frequency noise is expected to be governed by the noise characteristics of the master laser, while the slave laser dominates frequency noise at Fourier frequencies higher than the locking range.

3.3.5 Configuration of laser diodes and power supplies

Fiber delivery of the laser diodes light allows the laser diodes and their power supplies to be located at a distance from the laser itself. The multimode optical fiber has losses of 4 dB/km at 808 nm, so moving the laser diodes 100 meters from the laser will only reduce the power delivered by 5%. Each laser diode should deliver nominally 30 W of power and 40 diodes will be needed for the high power oscillator and 2 additional diodes are required for the intermediate power oscillator. If the diodes are powered with groups of 10 in series that means 4 power supplies will be required for pumping the high power stage. One additional power supply will be needed for the Peltier elements used for the laser diode temperature stabilization. This number of commercial power supplies could fit in a standard 19 in. rack that is 6 ft. tall. Each laser diode is controlled by a computer based PID controller, which results in a temperature-stability better than 20 mK. With this temperature-stability, additional noise resulting from variations of the total absorbed pump power due to pump wavelength changes can be neglected.

3.4 Summary of Anticipated Challenges

The most obvious challenge in the *Advanced LIGO* Laser design is the fundamental mode high power ring oscillator at an excellent beam quality. A further challenge is the injection locking scheme for frequency stabilization of the high power laser. Based on the above design principles, LZH has set up an injection locked high power laser with a master laser and two slave oscillators. The first results on this concept demonstrate a single frequency output power of nearly 190 W in a linear polarized fundamental mode operation. In the case of the auto lock function of the injection locking servo, relock times of less than 400 ms are realized.

References:

1. I.Zawischa PhD thesis

2. I. Zawischa *et al*., “The GEO 600 laser system,” Class.Quantum Grav. **19,** 1775-1781 (2002).

3. M.Frede at al., “High power fundamental mode Nd:YAG laser with efficient birefringence compensation”, Optics Express **12,** 3581-3589 (2004)

4. Maik Frede et al., “213 W linearly polarized fundamental mode Nd:YAG ring laser,“ in OSA Trends in Optics and Photonics (TOPS) Vol. 96, Conference on Lasers and Electro-Optics (CLEO), Technical Digest, Postconference Edition (Optical Society of America, Washington, DC, 2004), Paper CPDA2

4 Pre-modecleaner

4.1 Introduction

The pre-modecleaner (PMC) is a three mirror ring-cavity used for spatial filtering of the beam profile of the high power laser. The PMC is put into the main beam path and has to have a high transmissivity for the fraction of the light in the TEM_{00} mode. A length control system is needed to keep the cavity resonant with the incoming beam.

4.2 Requirements

We assume that the laser system meets its requirement to have less than 20 W of power in higher order modes. A trade off between spatial filtering and circulating power leads to an anticipated finesse of F=50.

The range of the PZT has to be large enough to compensate for the free-running length changes of the PMC spacer and its PZT actuator.

4.3 PMC design

The PMC design will be similar to the *Initial LIGO* PMC but with reduced finesse. The specifications of the PMC can be found in the table below:

Round trip length	0.42 m
Finesse	50 (s-pol)
Cavity linewidth	14 MHz
Higher order suppression	TEM_{01} (vertical): 200 TEM_{10} (horizontal): 780
Pointing relative to optical table	$\varepsilon_1 < (3\times10^{-5}/f)\sqrt{\text{Hz}} \quad f > 10\,\text{Hz}$
Actuator range	$\pm 2\,\mu\text{m}$
Actuator bandwidth	driven by gain requirement to not spoil power noise downstream
Beam waist size	$\omega_0 = 370\,\mu\text{m}$
Maximum Intensity	$1\ \text{MW}/\text{cm}^2$

The main purpose of the PMC is the spatial filtering of the high power laser beam. We assume that the higher order mode content of the laser is < 20 W.

The power in the TEM_{01} and TEM_{10} mode can be reduced by an automatic alignment system of the beam with respect to the relevant PSL reference which is the frame defined by the optical table. An easier way adopted for this conceptual design is to reduce the modal content of almost all higher order modes by the spatial filtering with a Fabry-Perot cavity. Once we have reliable measurements of the spatial profile of the high power laser, the spectral density of the spatial fluctuations and the motion of the optical table with respect to the suspended modecleaner we might revisit the use of an automatic alignment system.

A trade-off between spatial filtering and the maximum intensity on the PMC mirrors leads to the choice of a PMC finesse of 50. Once the spatial profile of the high power laser is known this choice needs to be checked in terms of sufficient spatial filtering for modes with $m+l > 2$. If the RF-RIN of the high power laser does not meet the requirements a higher PMC finesse or PMC length might be required to allow for RF-RIN filtering of the PMC. A careful analysis of thermal effects on the PMC mirrors will be needed to trade off spatial filtering, thermal loading RF-power filtering.

The length of the PMC will be controlled via a Pound-Drever-Hall scheme to make the PMC eigen-frequency to follow the frequency of the incident beam. The remaining difference between these frequencies will cause deviation of the phase and amplitude of the transmitted beam. The equivalent frequency noise on the transmitted beam will be reduced by the FSS which senses the beam downstream of the PMC. Implications of these coupled control loops need to be investigated. The amplitude noise on the transmitted beam that is caused by the non-perfect PMC length control should be less than the RIN at the error point of the second power stabilization loop (PSS2). This sets the required gain distribution for the PMC feedback loop. In case this requirement can not be met we need to investigate if the sensing point of PSS2 can be moved to a point downstream of the PMC.

To avoid acoustically driven length changes of the PMC and to keep the PMC mirrors clean and its transmission high, the PMC will be put into a sealed vessel. We need to investigate if mechanical isolation with respect to the optics table is needed to avoid acoustic coupling via this path. The pointing requirement of the PMC relative to the optical table needs to be kept in mind during such investigations. The vacuum requirements are driven by the required cleanliness. Information will be sought from experts if the laminar or molecular flow region is preferable.

5 Frequency Stabilization System

5.1 Overview

The principal performance requirements of the *Advanced LIGO* PSL frequency stabilization system fall into the following five categories:

- Long term (>100 sec) frequency stability
- Control band (0.1 – 10 Hz) frequency fluctuation levels
- GW band (10 Hz – 10 kHz) frequency noise levels
- Bandwidth and range of the *Wideband frequency input.*
- Range and response time of the *Tidal frequency input*

The first two requirement categories are new, while the last three are similar to, though generally less stringent than, the *Initial LIGO* requirements.

Although the *Advanced LIGO* laser source is different than the *Initial LIGO* laser, the NPRO (non-planar ring oscillator) master oscillator is similar to that utilized by the *Initial LIGO* laser, so we expect similar free-running frequency noise performance. The *Advanced LIGO* laser will utilize an NPRO manufactured by Innolight in Hanover, while the *Initial LIGO* laser utilizes an NPRO from Lightwave Electronics in Mountain View. Experience with the LZH injection-locked front-end laser shows that it does not add appreciable frequency noise to that of the NPRO oscillator. Furthermore, we do not expect a significant amount of additional frequency noise to be added by the final high-power slave resonator currently being developed at LZH.

The frequency stabilization scheme for the *Advanced LIGO* PSL is similar to that that employed for the *Initial LIGO* PSL except that the sample of the laser output directed to the reference cavity is picked off downstream of the pre-modecleaner. For the *Initial LIGO* PSL it is picked off upstream.

The global interferometer frequency stabilization scheme employs nested loops utilizing the increasing frequency sensitivity of three Fabry-Perot cavities; the PSL reference cavity, the IO mode-cleaner, and the interferometer's long arm cavities using the LSC common-mode signal. The PSL frequency stabilization sensor utilizes a linear, fixed-spacer reference cavity that is suspended on a vibration isolation system inside a vacuum chamber. The three frequency actuators are i) control of the master oscillator (NPRO) temperature, commonly referred to as the SLOW actuator, ii) a PZT bonded to the oscillator crystal that changes the frequency via strain-induced optical path length changes, commonly referred to as the FAST actuator, and iii) high-speed control of the optical phase via an electro-optic modulator located between the NPRO and the medium power stage.

A *wideband frequency input* actuator is provided to the IO detector subsystem for further stabilization of frequency fluctuations. This input shifts the frequency of the sampled beam directed to the reference cavity via an acousto-optic modulator (AOM) driven by a voltage-controlled oscillator (VCO). A *tidal frequency input* actuator is provided for very low-frequency correction via changes in the temperature of the reference cavity. Both of these actuators are similar in design to those utilized in the *Initial LIGO* PSL, and will of course utilize any improvements implemented during operation of the *Initial LIGO* PSL.

5.2 Long term frequency stability

The PSL frequency is required to be stable to within 100 kHz over time scales longer than 100 sec. At low frequencies, the laser frequency is locked to the resonance length of the fused silica reference cavity. The thermal expansion coefficient of fused silica is about 5×10^{-7} 1/K, so the long-term temperature stability of the reference cavity would have to be better than 0.5 mK.

While we have not attempted to measure this level of free-running stability, we have demonstrated the ability to reduce the effects of Earth tides by actuating on the temperature of the reference cavity. The performance of the tidal compensation system is discussed in the Tidal Input section, below.

5.3 Control band frequency fluctuation levels

The allowed frequency fluctuations in the control band, from 0.1 to 10 Hz, are summarized in Table 1, below.

Frequency band	Frequency stability req.
1 – 10 Hz	< 3 Hz-rms
0.4 – 1 Hz	< 100 Hz-rms
0.1 – 0.4 Hz	< 1000 Hz-rms

Table 1 Allowed frequency fluctuations in the control band.

The *Initial LIGO* PSL performance with respect to these requirements has not been measured. It is expected to be dominated by the length fluctuations of the reference cavity.

In a talk at the Aspen Conference (G050042-00) K. Numata analyzed the limits for frequency stabilization of a laser to a reference cavity. He analyzed the best results achieved by J. Berquist at NIST and the A. Brillet group in France with an ULE cavity. His results seem to indicate that the achieveble stability is limited by the thermal noise in the mirrors contacted to the spacer. Even though there are no out-of-loop measurement between 1Hz and 30Hz available a projection of the NIST and VIRGO results suggest that a frequency stability of about a factor of 10 better than the *Advanced LIGO* requirements could be achieved. (Probably even better as the Q factor of fused silica is better than that of ULE). Care has to be taken that frequency noise caused by a Doppler shift associated with length fluctuations in the reference cavity path and noise introduced by the AOM is small enough to achieve the requirements.

5.4 GW band frequency noise levels

The required frequency noise levels in the GW band are shown by the blue lines in Figure 12, below. The *Initial LIGO* requirement is shown by the green lines. Note that above 100 Hz the *Advanced LIGO* requirements have been relaxed by a factor of two and that they extend down to 10 Hz rather than 40 Hz as for *Initial LIGO*.

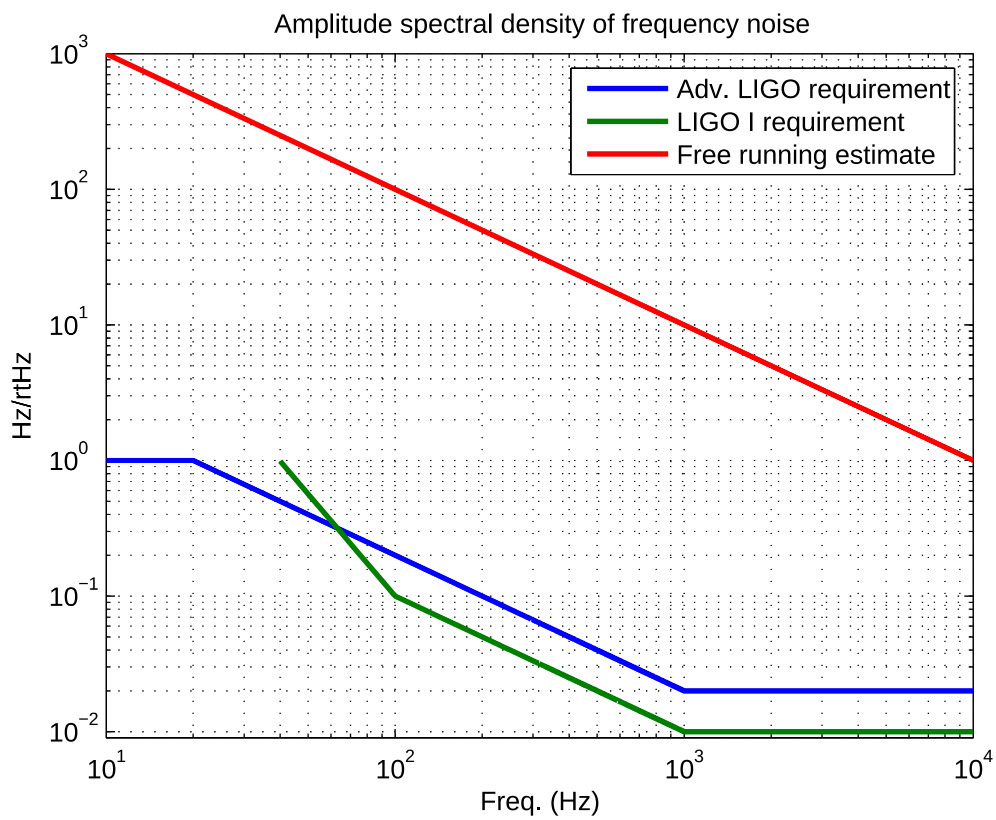

Figure 12. PSL free-running frequency noise estimate and *Advanced LIGO* and *Initial LIGO* frequency noise requirements.

It is expected that the free running frequency noise of the *Advanced LIGO* laser will be dominated by the free running frequency noise of the NPRO. This assumption can be (and should be) verified by a beat measurement between a fraction of the light sampled downstream of the high power stage and the light from the NPRO. The InnoLight NPRO is similar in design to that of the Lightwave NPRO, so we expect that the free running noise performance will be similar as well. The typical amplitude spectral density of the frequency noise of a free running NPRO can be approximated by $10\ \mathrm{kHz}/f\ \ 1/\sqrt{\mathrm{Hz}}$, where f is the frequency of interest. This estimate of the free-running laser frequency noise is plotted in Figure 12 (red line).

Because we expect the free-running frequency noise to be similar to that of the *Initial LIGO* PSL laser, and because the frequency stabilization sensor and actuators are similar to those in the *Initial LIGO* PSL, the required control loop performance is also similar to what was needed for *Initial LIGO*. We assume that all performance enhancements implemented in the *Initial LIGO* PSLs during commissioning and operation of *Initial LIGO* will be applied to the *Advanced LIGO* PSL. The open-loop transfer function of the FSS operating in the LIGO H1 interferometer[1] was

---

[1] The FSS operating on the H1 system at the time of the measurements is referred to as the Table-top frequency stabilization servo (TTFSS). It is based on a revised FSS that is described in a document that can be found at http://www.ligo.caltech.edu/docs/T/T030076-00.pdf. The TTFSS servo electronics are located on the PSL table, close

measured in December, 2004 and is shown in Figure 13 (blue curve). Based on the estimate of the free-running frequency noise and the required suppressed frequency noise level (see Figure 12) we can estimate the required loop gain as shown by the green line in Figure 13. The measured loop gain exceeds the requirement by at least 10 dB at all frequencies.

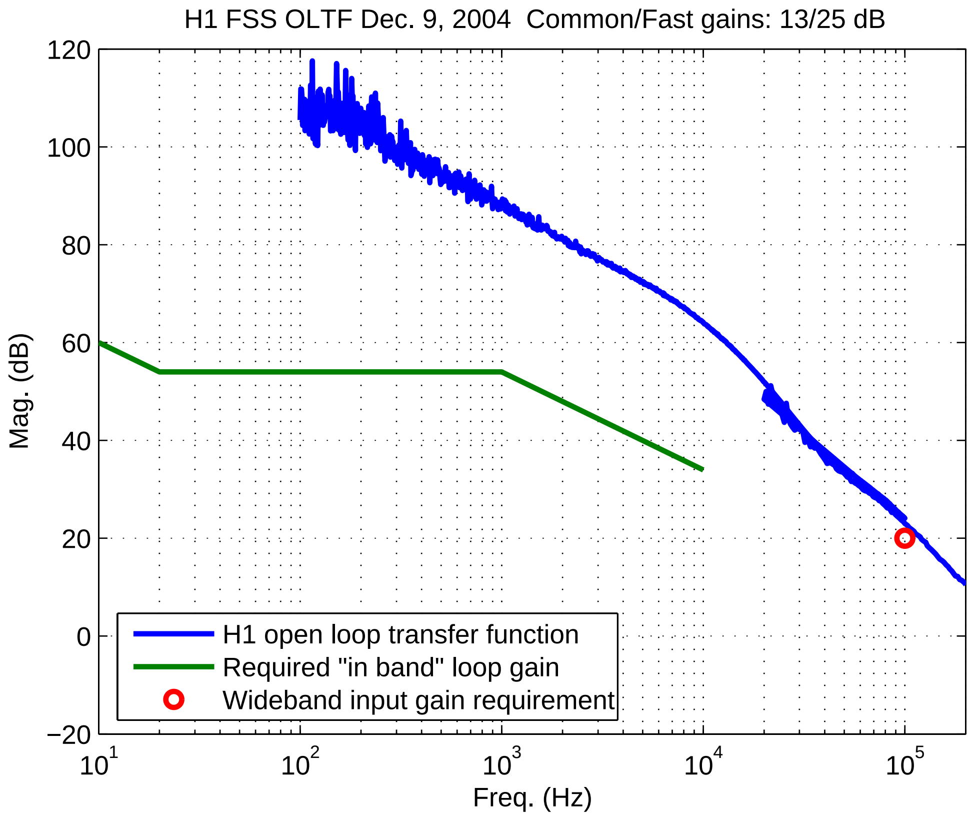

Figure 13. Measured FSS open loop transfer function and gain required to meet the suppressed frequency noise requirement. Based on assumed free-running frequency noise.

Figure 14 shows the LIGO H1 PSL frequency noise measured by the 15-m suspended modecleaner on Oct. 2, 2004. This is an upper limit on the PSL frequency noise because it is the noise sensed by the modecleaner servo and includes modecleaner length and sensing noise as well as noise that might be added by the IOO optical components between the PSL/IOO interface point and the modecleaner. These include the three IOO EOMs, the adjustable half wave plate and polarizing optics for power adjustment, and the IOO periscope. The solid green lines represent the *Advanced LIGO* PSL frequency noise requirements and the red lines are the *Initial LIGO* requirements. Note that except for a number of sharp peaks, which appear to be of acoustic origin, the *Initial LIGO* PSL meets the *Advanced LIGO* frequency noise requirements.

---

to the laser frequency actuators, and control and monitoring signals interface with the TTFSS module via an interface board situated in the Euro-card crate in the PSL electronics rack. The LIGO drawing numbers for the relevant electronics schematics are D040105 (Tabletop Frequency Stabilization Servo), D040423 (TTFSS Interface Board) and D040469 (RF Summing Box).

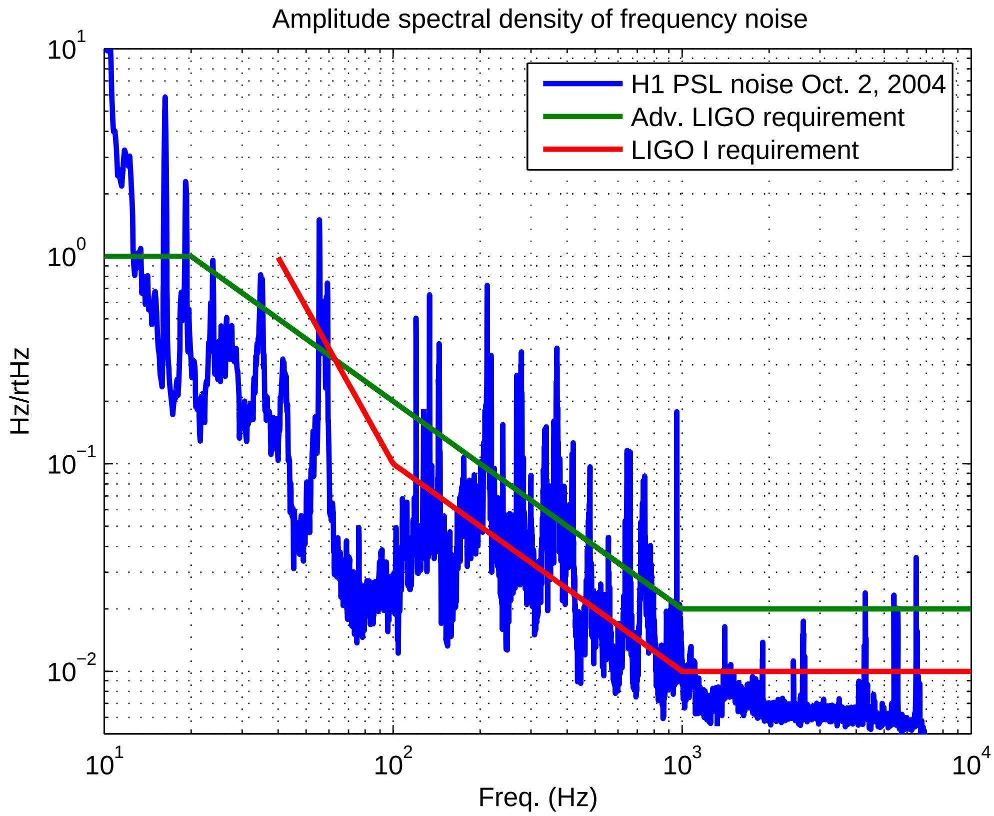

Figure 14: LIGO H1 PSL frequency noise performance measured by the 15-m-long suspended modecleaner on Oct. 2, 2004.

One difference between the *Advanced LIGO* and the *Initial LIGO* FSS schemes is that for *Advanced LIGO* the beam directed toward the reference cavity is sampled **after** the PMC rather than **before** the PMC as in the *Initial LIGO* PSL. This scheme has the benefits that the beam directed to the FSS has been spatially filtered by the PMC and that frequency noise added by the PMC is suppressed by the FSS loop. However, because the PMC can introduce frequency changes as the length of the PMC is varied, the frequency control loop is coupled to the PMC length control loop.

A TTFSS was installed in the LASTI Lab at MIT in which the frequency servo sample beam is picked off downstream of a PMC cavity with a pole frequency of 1.6 MHz[2]. The loop locks easily and preliminary measurements indicate that the unity gain frequency is around 500 kHz, but detailed measurements have not yet been made. We expect more concrete results early in 2005[3].

---

[2] Note that the *Advanced LIGO* PSL PMC pole will be at approximately 7 MHz, reducing its influence on the FSS performance.

[3] Private communication with David Ottaway.

5.5 Wideband frequency input

The requirements for the *wideband frequency input* are summarized in Table 2, below.

Wideband frequency input	
Bandwidth	100 kHz: less than 20 degrees phase lag at 100 kHz
Range:	DC-1 Hz: 1 MHz pk-pk
	f > 1 Hz: 10 kHz pk-pk

Table 2 Wideband frequency input performance requirements.

The *Advanced LIGO* PSL will utilize the same VCO as that utilized for the *Initial LIGO* PSL. The requirements allow for a reduction in the VCO range by a factor of ten. A re-designed VCO with ten times smaller range should have less noise, but, especially considering that the *Advanced LIGO* high frequency noise requirements have been relaxed by a factor of two, we expect to meet the frequency noise performance with the existing VCO.

The gain and phase lag requirement at 20 kHz translates into a required loop gain of at least 20 dB at 100 kHz for the frequency stabilization. As shown in Figure 13, the *Initial LIGO* TTFSS meets this requirement.

5.6 Tidal frequency input

The requirements for the *tidal frequency input* are given in Table 3.

Range: 50 MHz pk-pk
Speed: time constant < 20 min

Table 3 *Tidal frequency input* performance requirements.

The hardware and electronics for the *Advanced LIGO tidal frequency actuator* are identical to those utilized for *Initial LIGO*. Frequency changes are realized by changing the temperature of the reference cavity to which the laser frequency is locked. The temperature of the reference cavity is varied via changes in the temperature of the stainless steel vacuum chamber in which the reference is suspended.

At Hanford, a computer model is used to predict the tidal stretching along the interferometer arms. This model, together with empirical estimates of the response of the reference cavity to changes in the temperature of the vacuum enclosure, is used to generate a time series of predicted vacuum chamber temperatures. With the predicted temperatures fed to the reference cavity vacuum chamber temperature controller, long lock stretches enable determination of the degree of tidal compensation achieved. This is accomplished by monitoring the residual drive to the end test mass fine actuators required to relieve the drive on the suspension controllers.

The common and differential tidal predictions and the residual length corrections required after the predicted correction has been applied to the *tidal frequency input* are shown in Figure 15. Note that the residual common mode tidal effect has been reduced by about a factor of four from roughly 90 μm p-p to about 20 μm p-p.

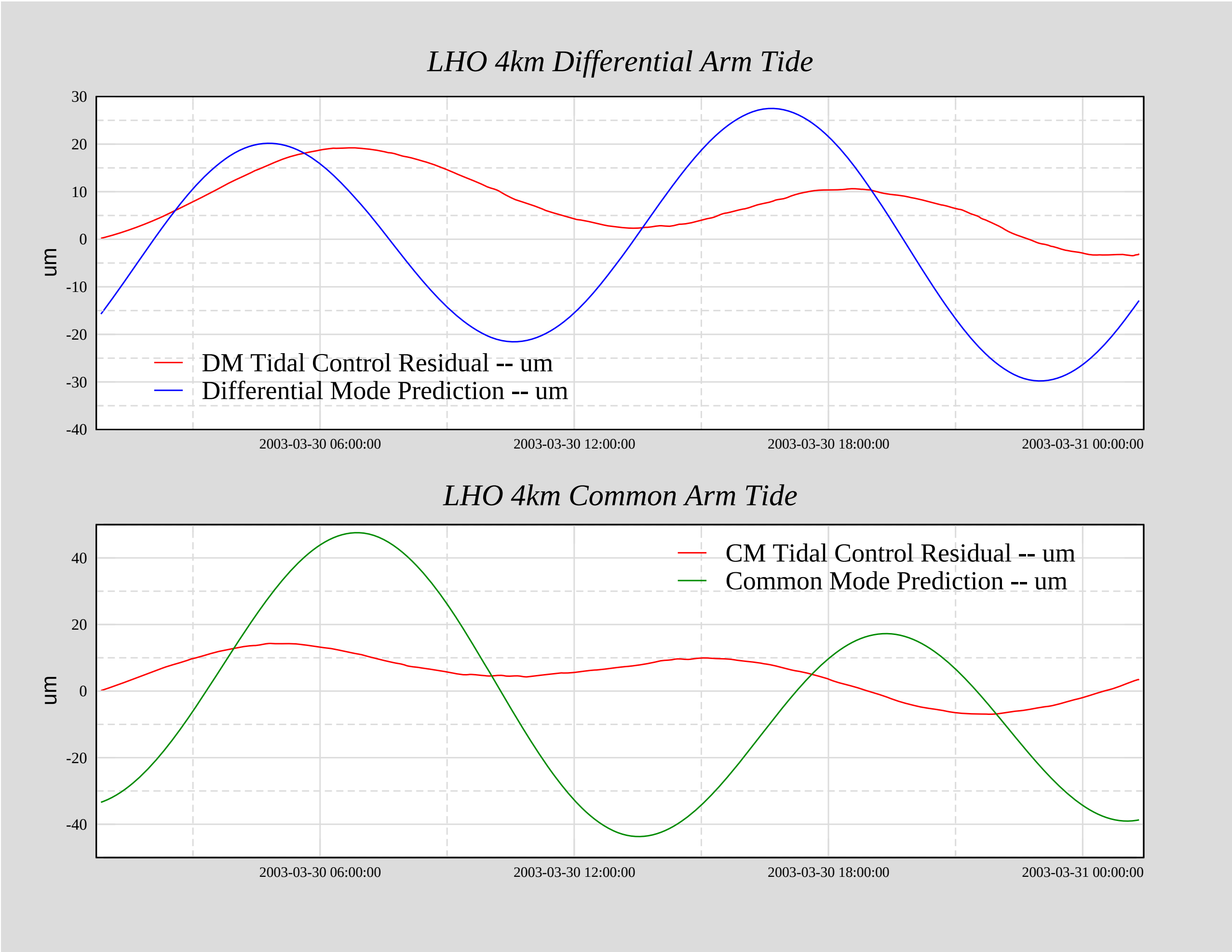

Figure 15. Performance of the LIGO H1 tidal compensation system.

While the present system routinely compensates for 50-75% of the common-mode tidal stretching, the time constant for the reference cavity temperature actuation is much longer than the design requirement. This time constant has proved difficult to measure, but the present best estimate is 270 minutes. Furthermore, the response has been found to differ from a single low frequency pole. This is believed to be due to the much longer time constant for temperature changes to propagate from the vacuum chamber walls through the massive stainless steel plates of the vibration isolation stack to the top plate which occludes approximately 25% of the solid angle seen by the reference cavity. During the course of two student research (SURF) projects, an upgrade to the present design that gave much better temperature stability, although little improvement in the response time, was designed and tested. This upgrade, which basically consists of a temperature-controlled copper shroud inside the reference cavity vacuum chamber, could be implemented fairly easily and inexpensively, if required.

6 Intensity Stabilization

A number of table-top experiments within the gravitational-wave community have achieved relative intensity noise figures of $(1-5)\times 10^{-8}\ 1/\sqrt{\text{Hz}}$ at the frequencies of interest. These experiments have seemingly highlighted the importance of beam jitter on the photodiode, the effects of acoustics and of dust particles in the optical path to the photodetector. All experiments have had ample electronic gain to suppress the relative intensity noise beyond their target levels but a discrepancy always exists between the photodetector used by the intensity stabilization electronics and an independent photodetector. The discrepancy is more apparent at low frequencies and the causes of the discrepancy are under active research. The intensity stabilization of the PSL is expected to be a major challenge. Figure 16 shows the best relative intensity noise result achieved to date at 10 Hz with *Initial LIGO*.

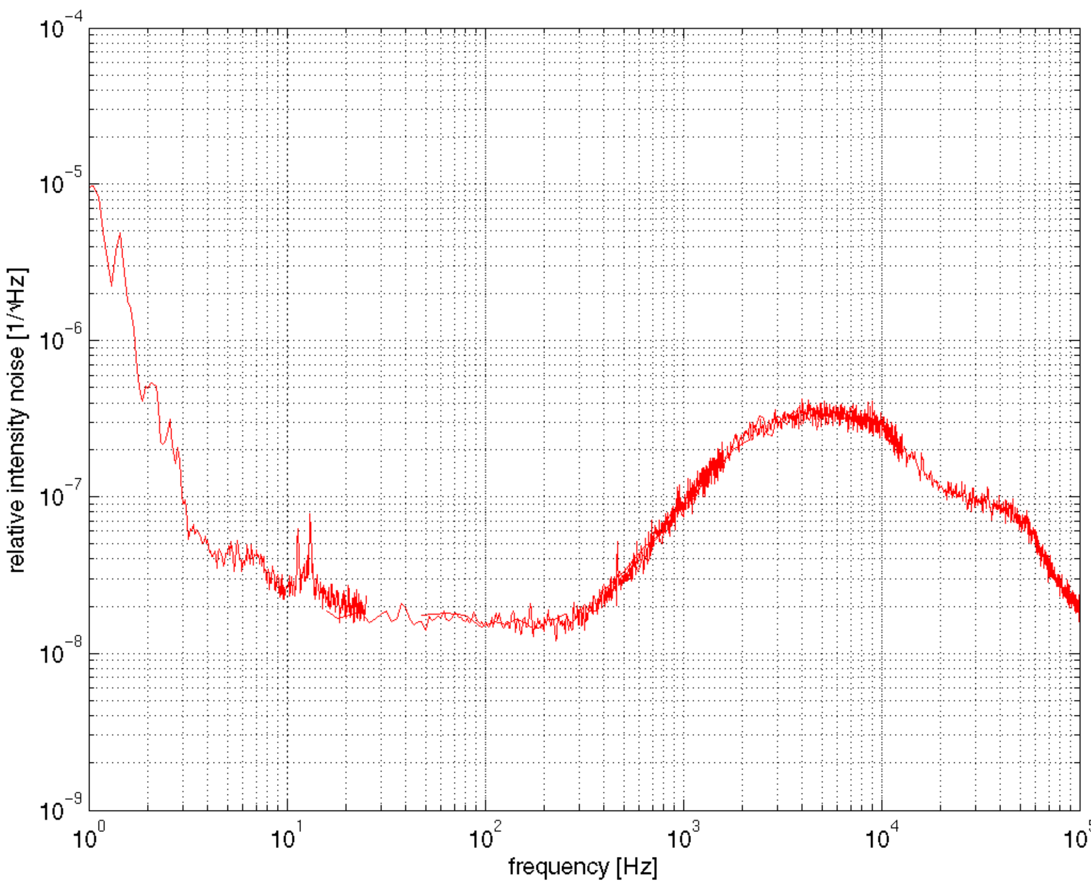

Figure 16. The relative intensity noise as measured by an out of loop photodetector located after the suspended modecleaner at LIGO Livingston.

At the time of writing the intensity stabilization for *Initial LIGO* is currently being commissioned with the active photodetector being located before the suspended modecleaner and with provision for a photodetector located after the suspended modecleaner. Experience gained with *Initial LIGO* will be used in determining the ultimate location for the photodetector topology used in *Advanced LIGO*. If a dual photodetector topology is to be retained then an anticipated challenge would be the seamless transition from one photodetector to another as this might introduce small offsets which would cause the high gain servo to saturate. Nested loops with an AC coupled outer-loop might overcome this problem.

6.1 Low Frequency Intensity Variations

The requirement for low-frequency power stability is that the intensity fluctuations should be less than 5% peak-to-peak over any 24-hour period without intervention. In addition, there is a requirement that there be an input to the PSL that would enable stabilization to a level of 1% peak-to-peak for time scales longer than 10 s to 24 hours.

This is expected to be achieved via a software control loop that periodically monitors the PSL output power and adjusts the pump diode current accordingly. Whilst this has not been fully implemented with the *Initial LIGO* PSL, preliminary testing suggests that this approach is satisfactory.

6.2 Control Band Fluctuations

The control band is defined as the frequency range from 0.1 to 10 Hz. The relative intensity noise requirements for this band are summarized in the following table.

Frequency [Hz]	$\delta P_{\mathrm{rms}} / P$
0.1 to 0.4	$< 10^{-3}$
0.4 to 10	$< 10^{-4}$

6.3 Fractional Light Intensity Fluctuations in the GW Band

The PSL intensity noise requirement at the input to the interferometer is summarized in the following table.

Frequency [Hz]	**Requirement** [$1/\sqrt{\mathrm{Hz}}$]
10	2×10^{-9}
$10 < f < 500$	$2\times10^{-10}\left(f/\mathrm{Hz}\right)$
$f \geq 500$	1×10^{-7}

The actuator to be used for the intensity stabilization is expected to be some form of current shunt similar to that employed in the *Initial LIGO* PSL. This would allow for fast modulation of a sample of the pump diode current rather than modulation of the entire pump diode current.

6.3.1 High Power Photodetector

The photocurrent required to achieve a shot-noise limited relative intensity noise of $2\times10^{-9}\ 1/\sqrt{\text{Hz}}$ is only 80 mA. Photodetectors capable of handling that level of photocurrent are readily available, though not commercially. For example the RF photodetector employed in *Initial LIGO* is capable of handling a maximum photocurrent of 150 mA. Other designs exist capable of handling even higher photocurrents. Within the LIGO Laboratory, handling a photocurrent greater than 500 mA has been demonstrated albeit for relatively short periods of time (approximately 10 hours).

A concern with the photodetector would be the spatial uniformity across the surface of the photodiode and its affect on the photodetector response. Each photodiode would have to be carefully characterized before being incorporated into a high power photodetector.

A possible limit on the performance of the intensity stabilization would be the beam pointing caused by the relative motion between the modecleaner and the high power photodetector. To minimize this effect, the strawman plan is to locate both the in-the-loop and out-of-loop photodetector on the same seismic platform as the suspended modecleaner. Further isolation from the ground motion would be afforded by having the photodetector suspended. The suspension requirements of the photodetector have yet to be worked out. Being located on the same seismic platform as the modecleaner forces the high power photodetector to be compatible with the LIGO vacuum standards as the photodetector would be located within the LIGO vacuum system. This places a reliability requirement on the photodetector since replacing a bad unit would entail going into the vacuum system, resulting in interferometer down time. Each high power photodetector would have to undergo some level of in-vacuum and simultaneous high power qualification.

6.4 Fractional Light Intensity Fluctuations in the RF Band

For frequencies greater than 9 MHz the relative intensity noise must be less than 3 dB above the shot noise for a detected photocurrent of 50 mA. In case this requirement is not met by the *Advanced LIGO* laser passive filtering could be provided by the spatial cavity filter illustrated in Figure 2. By appropriate choice of cavity finesse, the amount of filtering can be adjusted. Should the circulating intensity be too high for the mirror coatings, two low-finesse spatial cavity filters can be deployed. A challenge would be to make such a spatial filter cavity with a high power throughput. To date typical power throughputs are around 85-90%.

6.5 Summary of Anticipated Challenges

Undoubtedly the greatest challenge is the relative intensity noise requirement at 10 Hz. To date the best reported level of stabilization achieved at 10 Hz has been $1\times10^{-8}\ 1/\sqrt{\text{Hz}}$ in an experiment at MIT (J. Rollins *et al*.) and $1\times10^{-8}\ 1/\sqrt{\text{Hz}}$ at 20Hz in an experiment in Hanover (Seifert *et al*.). Both measurements were out-of-loop measurements. The Hanover measurement was performed downstream of a PMC on a photodiode in vacuum. (This photodetector does not meet the *Advanced LIGO* vacuum requirements).

Experiments are underway to understand the limiting noise sources in the power noise sensing.